New Journal of Physics
The open access journal at the forefront of physics

Deutsche Physikalische Gesellschaft DPG IOP Institute of Physics

PAPER • OPEN ACCESS

Process of equilibration in many-body isolated systems: diagonal versus thermodynamic entropy

To cite this article: Samy Mailoud *et al* 2020 *New J. Phys.* **22** 083087

New Journal of Physics
The open access journal at the forefront of physics

Deutsche Physikalische Gesellschaft DPG
IOP Institute of Physics

Published in partnership with: Deutsche Physikalische Gesellschaft and the Institute of Physics

OPEN ACCESS

RECEIVED
18 March 2020

REVISED
9 July 2020

ACCEPTED FOR PUBLICATION
15 July 2020

PUBLISHED
28 August 2020

PAPER

Process of equilibration in many-body isolated systems: diagonal versus thermodynamic entropy

Samy Mailoud[1], **Fausto Borgonovi**[2,3] **and Felix M Izrailev**[1,4]

[1] Instituto de Física, Benemérita Universidad Autónoma de Puebla, Apartado Postal J-48, Puebla 72570, Mexico
[2] Dipartimento di Matematica e Fisica and Interdisciplinary Laboratories for Advanced Materials Physics, Università Cattolica, via Musei 41, 25121 Brescia, Italy
[3] Istituto Nazionale di Fisica Nucleare, Sezione di Pavia, via Bassi 6, I-27100, Pavia, Italy
[4] NSCL and Department of Physics and Astronomy, Michigan State University, E Lansing, Michigan 48824-1321, United States of America

E-mail: samy.mailoud90@gmail.com

Keywords: thermalization, isolated quantum many-body systems, quantum chaos

Abstract

As recently manifested [1], the quench dynamics of isolated quantum systems consisting of a finite number of particles, is characterized by an exponential spreading of wave packets in the many-body Hilbert space. This happens when the inter-particle interaction is strong enough, thus resulting in a chaotic structure of the many-body eigenstates considered in the non-interacting basis. The semi-analytical approach used here, allows one to estimate the rate of the exponential growth as well as the relaxation time, after which the equilibration (thermalization) emerges. The key ingredient parameter in the description of this process is the width Γ of the local density of states (LDoS) defined by the initially excited state, the number of particles and the interaction strength. In this paper we show that apart from the meaning of Γ as the decay rate of survival probability, the width of the LDoS is directly related to the diagonal entropy and the latter can be linked to the thermodynamic entropy of a system equilibrium state emerging after the complete relaxation. The analytical expression relating the two entropies is derived phenomenologically and numerically confirmed in a model of bosons with random two-body interaction, as well as in a deterministic model which becomes completely integrable in the continuous limit.

1. Introduction

The problem of thermalization in isolated quantum systems remains a hot topic in the field of modern statistical mechanics. It has been shown since long that thermalization can emerge without the presence of a heat bath, even if the number of interacting particles is small [2–7]. One of the main problems in this field is to establish the conditions under which a given system manifests strong statistical properties, such as the relaxation to equilibrium. Due to a remarkable progress in the study of this and related problems, much is already understood in theoretical and numerical approaches (see [8–12] and references therein) as well as in experimental studies of interacting particles in optical traps [13–17], even if many basic problems still need further intensive efforts.

As was shown in reference [18], the mechanism for the onset of statistical behavior for a quantum isolated system is the chaotic structure of the many-body eigenstates in a given basis defined in absence of inter-particle interaction. As for the properties of eigenvalues (such as the Wigner–Dyson type of the nearest-neighbor level spacings distribution), it was shown [19, 20] that they have a little impact on the global statistical properties of the wave packet dynamics.

The concept of chaotic eigenstates originates from random matrix theory (RMT), which was suggested by Wigner in order to explain local properties of energy spectra of heavy nuclei, observed experimentally [21, 22]. Being unable to describe global properties of energy spectra of complex physical systems, the random matrices turned out to be effective models for the description of the local statistical properties of

spectra, that were predicted and later confirmed experimentally to be universal. Since long time, the RMT has served as the theory of quantum chaos with strong chaotic properties.

Next steps in the mathematical study of many-body chaotic systems were performed by taking into account the typical two-body nature of the inter-particle interaction. As a result, a new kind of random matrix model, closer to the physical realm than the RMT and known as the two-body random interaction (TBRI) model has been invented [23–25]. In contrast with the standard RMT, it depends on additional physical parameters, such as the number of interacting particles and the strength of inter-particle interaction. In these matrices a complete randomness is embedded into the two-body matrix elements, from which the many-body matrix elements are constructed.

A distinctive property of the TBRI matrices (in application to both Fermi and Bose particles) is that they are non-ergodic in the sense that the averaging inside a matrix is not equal to the ensemble averaging, even for a very large matrix size [26]. Moreover, these matrices are banded-like, sparse and non-invariant under rotations so that all their properties are related to a specifically given non-interacting basis. For this reason, rigorous analytical analysis (especially, for a finite number of particles) is strongly restricted and many results can be obtained only numerically.

To date, the TBRI matrices are extensively studied, however, mainly in what concerns the properties of energy spectra and structure of eigenstates (see for instance [26–30] and references therein). As for the related time evolution, a close attention to this problem was recently surged ahead by the increasing interest to the problem of scrambling, understood as the loss of information in the process of equilibration and thermalization. Further progress in random matrix theories was achieved due to remarkable results based on the Sachdev–Ye–Kitaev (SYK) model [31, 32], which can be considered as a variant of the TBRI model (see, for instance, reference [33]). The SYK model has attracted much attention in recent years, widely used as an effective model for two-dimensional gravity, also in application to black holes [34–36]. For the latter problem, a particular interest has been given to the spreading and disappearing of information in the process of thermalization.

As is known, chaos in classical systems is originated from the exponential sensitivity of motion with respect to small perturbations. As a result, the distance in the phase space between two close trajectories increases, in average, exponentially fast and the rate of such an instability is given by the largest Lyapunov exponent λ. In quantum systems, this mechanism is absent due to the linear nature of the Schrödinger equation. Although for quantum systems with a strongly chaotic classical limit, one can observe a complete correspondence to the classical behavior, the time scale $t \sim 1/\lambda$ on which it happens, was found to be dramatically short due to the fast spreading of the wave function. As a result, the chaotic behavior of quantum observables is suppressed in time.

As for quantum systems without classical limit, even in the presence of strong disordered potentials, observation of exponential instability in the quantum motion was questioned for a long time. However, recent remarkable progresses have led to the discovery of the out-of-time-order correlators (OTOC), which are four-point correlation functions with a specific time ordering. Extensive studies have manifested the effectiveness of the OTOC in application to various physical systems [37–40].

It is widely believed that OTOCs can solve the problem of thermalization, however, this is not obvious since their exponential growth in time is bounded by a time scale which cannot be associated with the complete relaxation to equilibrium [41]. Indeed, typical applications of OTOC are mainly restricted by *local* observables, in contrast with the very point that thermalization is a *global* concept. The situation reminds that which was thoroughly discussed in the early stage of the setting up of the classical chaos theory. Specifically, for some time it was believed that correlation functions should typically manifest an exponential time decrease. Unexpectedly, it was found later that realistic physical systems, even if strongly chaotic, are typically characterized by a quite slow decrease of correlations. Also, an infinite number of correlations functions can be defined and their time behavior can be in principle very different. Thus, even if serving as a good test for the instability of quantum many-body systems, the direct relevance of the OTOC to the time scale of thermalization remains questionable.

One of the first attempts to relate the OTOC to the long-time dynamics in many-body systems has been performed in reference [42]. Specifically, it was asked whether OTOC can describe the exponential long-time growth of the effective number $N_{\rm pc}$ of components of the wave function in the process of a complete equilibration. This number can be estimated via the *participation ratio* provided the many-body eigenstates can be considered strongly chaotic. An important result of this study is that there are two characteristic time scales, one of which is directly related to the survival probability and can be defined in terms of the Lyapunov exponent, therefore, in terms of the OTOC. However, a complete thermalization is described by the excitation flow along a kind of network created by the many-body states. An application of OTOC to such type of dynamics [42] has shown that $N_{\rm pc}$ can be presented as a set of the OTOCs, each of them describing an excitation on a specific time scale, due to standard perturbation theory. For a finite

number of many-body states, this process terminates when all states are excited, which create an energy shell in the Hilbert space (for details see [18]).

Numerical data obtained for the TBRI model with a finite number of bosons occupying a number of single-particle energy levels [1], as well as for models of a finite number of interacting spins-1/2 in a finite length chain [19, 20], clearly demonstrated that, in presence of chaotic eigenstates, the global time behavior of the systems is very similar. One has to note that even if one of the spin models is integrable, with a Poisson-like level spacing distribution, this does not influence the quench dynamics. These results confirm the prediction that for many-body systems the type of energy level fluctuations is less important than the chaotic structure of the many-body states.

In this paper we continue the study of the quench dynamics, paying attention to the new question of the relevance between the diagonal entropy related to an initially excited state, and the thermodynamic entropy emerging in the process of thermalization. We show numerically and describe semi-analytically that there is a one-to-one correspondence between them, with some corrections due to the different size between interacting and non-interacting energy spectra. This remarkable result holds both for the TBRI model with finite number of bosons, and for the model originated from the celebrated Lieb–Liniger (LL) model [43–45]. The latter model, which has no random parameters, was proved to be integrable with the use of Bethe ansatz.

The LL model describes one-dimensional (1D) bosons on a circle interacting with a two-body point-like interaction. It belongs to a peculiar class of quantum integrable models solved by the Bethe ansatz [46, 47]; in particular, it possible to show that it has an infinite number of conserved quantities. Apart from the theoretical interest, this model is important in view of various experiments with atomic gases [48–50]. For a weak inter-particle interaction the LL model can be described in the mean-field (MF) approximation. Contrarily, for a strong interaction, the 1D atomic gas enters the so-called Tonks–Girardeau (TG) regime in which the density of the interacting bosons becomes identical to that of non-interacting fermions (keeping, however, the bosonic symmetry for the wave function) [45]. The crossover from one regime to the other is governed by the ratio n/g between the boson density n and the interaction strength g. The latter constant is inversely proportional to the 1D inter-atomic scattering length and can be experimentally tuned with the use of the Feshbach resonance (see, for example, [51] and references therein). Specifically, the MF regime occurs for $n/g \gg 1$ and the TG regime emerges for $n/g \ll 1$ [45].

In our numerical study, we consider a *finite* many-body Hilbert space by fixing the total number of momentum states and the number N of interacting bosons. This truncated Lieb–Liniger model (t-LL) allows one to correctly obtain both the eigenvalues and many-body eigenstates of the original LL model, in a given range of energy spectrum [52]. This method (truncation of the infinite spectrum) can be considered as the complimentary one to the recently suggested way [53], according to which a finite number of eigenstates involving into the quench dynamics is used.

2. Quench dynamics

Below, we study the quench dynamics in two different models described by the Hamiltonians written as

$$H = H_0 + V. \tag{1}$$

Here the first term H_0 describes N non-interacting identical bosons occupying M single-particle levels specified by the energies ϵ_s,

$$H_0 = \sum \epsilon_s \hat{n}_s, \tag{2}$$

while the second term V stands for the two-body interaction between the particles,

$$V = \sum V_{s_1 s_2 s_3 s_4}\, a^\dagger_{s_1} a^\dagger_{s_2} a_{s_3} a_{s_4}. \tag{3}$$

Here $\hat{n}_s = \hat{a}^\dagger_s \hat{a}_s$ is the number of particles in the corresponding $s-$level, with $\hat{a}^\dagger_s$ and $\hat{a}_s$ as the creation/annihilation operators acting on the sth level, and the two-body matrix elements $V_{s_1 s_2 s_3 s_4}$ specify the type and strength of the inter-particle interaction. The interaction conserves the number of bosons and connects many-body states that differ by the exchange of at most two particles. Due to the two-body nature of the interaction, the matrix elements $H_{ij} = \langle i|H|j\rangle$ are non-zero only when the two non-interacting many-body basis states $|i\rangle$ and $|j\rangle$ have single-particle occupations which differ by no more than two units. This means that the Hamiltonian matrix is sparse which is a common property of realistic many-body systems.

Our aim is to compare the dynamical properties of two models:

(a) the TBRI model with completely random and independent values of $V_{s_1 s_2 s_3 s_4}$

(b) the t-LL model which is deterministic (without random parameters) and integrable in the limit $M \to \infty$.

The non-interacting many-body eigenstates $|k\rangle$ (basis states) of

$$H_0 = \sum_k \mathcal{E}_k \, |k\rangle \, \langle k|$$

are obtained by creating N bosons in M single-particles energy levels, so that $|k\rangle = a^\dagger_{s_1} \ldots a^\dagger_{s_N}|0\rangle$, where $1 \leqslant s_1, \ldots, s_N \leqslant M$. In this way, we determine the non-interacting many-particles basis, in which the Hamiltonian is a diagonal matrix. As a result, the many-body eigenstates $|\alpha\rangle$ of the total Hamiltonian H are represented in terms of the basis states $|k\rangle$ as

$$|\alpha\rangle = \sum_k C^\alpha_k \, |k\rangle \, , \tag{4}$$

where C^α_k are obtained by exact numerical diagonalization. Below we use Latin letters when referring to the non-interacting basis of H_0, while Greek ones stand for the basis of H.

After specifying the non-interacting basis $|k\rangle$, one can study the wave packet dynamics in this basis, after switching on the two-body interaction V. Our analytical and numerical results refer to the situation when initially the system is prepared in a particular eigenstate of H_0,

$$|k_0\rangle = \sum_\alpha C^\alpha_{k_0} \, |\alpha\rangle \, . \tag{5}$$

and evolved according to the full interacting Hamiltonian H. To do this, we focus on the time dependence of the effective number $N_{\rm pc}(t)$ of principal components of the wave function,

$$N_{\rm pc}(t) \equiv \left(\sum_k |\langle k|\mathrm{e}^{-\mathrm{i}Ht}|k_0\rangle|^4 \right)^{-1} , \tag{6}$$

known in literature as the *participation ratio*.

In terms of eigenvalues and many-body eigenstates of the Hamiltonian H the participation ratio can be presented as

$$N_{\rm pc}(t) = \left\{ \sum_k \left[P^d_k + P^f_k(t) \right]^2 \right\}^{-1} , \tag{7}$$

where

$$P^d_k = \sum_\alpha |C^\alpha_{k_0}|^2 |C^\alpha_k|^2 \tag{8}$$

and

$$P^f_k(t) = \sum_{\alpha \neq \beta} C^\alpha_{k_0} C^{\alpha *}_k C^\beta_{k_0} C^{\beta *}_k \mathrm{e}^{-\mathrm{i}(E^\beta - E^\alpha)t} \tag{9}$$

are the diagonal and off-diagonal parts of

$$P_k(t) = |\langle k|\mathrm{e}^{-\mathrm{i}Ht}|k_0\rangle|^2 = \sum_{\alpha,\beta} C^{\alpha *}_{k_0} C^\alpha_k C^\beta_{k_0} C^{\beta *}_k \mathrm{e}^{-\mathrm{i}(E^\beta - E^\alpha)t} . \tag{10}$$

As was recently shown for different models with chaotic behavior [1], the number $N_{\rm pc}$ increases exponentially fast in time, provided the eigenstates involved in the dynamics, are strongly chaotic. After some relaxation time t_s, the value of $N_{\rm pc}$ fluctuates around the saturation value due to the complete filling of a portion of the total Hilbert space, called energy shell. Such a wave packet dynamics occurs when the many-body eigenstates of H are fully delocalized in the energy shell. This scenario explains the basic properties of the quench dynamics, before and after the saturation.

3. Semi-analytical approach

The semi-analytical approach developed in [4] for TBRI matrices with an infinite number of interacting Fermi-particles and modified in [1] for finite Bose-systems, allows one to obtain simple estimates for two

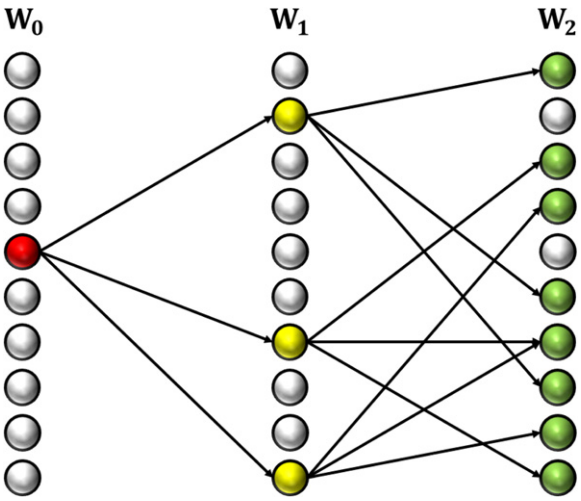

Figure 1. Probability flow in the many-body Hilbert space with the connectivity $\mathcal{K} = 3$.

important characteristics of the quench dynamics. The first characteristic is the rate of the exponential growth for the $N_{\rm pc}(t)$. The second characteristic is the time scale t_s on which the exponential growth of $N_{\rm pc}(t)$ occurs.

The two above characteristics can be estimated with the use of the semi-analytical approach originally developed in [54] for an infinite number of particles. To start with, we write down an infinite set of probability conservation equations, used for the description of the probability flow $W(t)$ in the many-body Hilbert space of H_0. To this end, let us consider an initial non-interacting state $|k_0\rangle$, and the probability $W_0(t)$ to be in this state at the time t. Correspondingly, we define the set $\mathcal{M}_0 = \{|k_0\rangle\}$ consisting of the initial state alone. In order to describe how the probability spreads in time we consider all states $|k_i\rangle$ directly coupled to the initial one via the two-body interaction V. We call this set $\mathcal{M}_1 = \{|k_i\rangle$ for which $|\langle k_0|V|k_i|\rangle \neq 0\}$. From this set we define $W_1(t)$ as the probability to be in $\mathcal{M}_1$ at the time t. As time increases, the probability flows onto another set $\mathcal{M}_2$ (with probability W_2) consisting of those states, coupled with the states of $\mathcal{M}_1$ by non-zero Hamiltonian matrix elements and so on (see figure 1). Neglecting the backward flow the infinite set of rate equations reads,

$$\begin{aligned} \frac{{\rm d}W_0}{{\rm d}t} &= -\Gamma W_0, \\ \frac{{\rm d}W_1}{{\rm d}t} &= -\Gamma W_1 + \Gamma W_0, \\ \frac{{\rm d}W_2}{{\rm d}t} &= -\Gamma W_2 + \Gamma W_1, \\ &\cdots \end{aligned} \tag{11}$$

where we have introduced the parameter Γ describing the exponential decay rate of the initial probability $W_0(t) \equiv P_{k_0}(t)$. In reference [54] it was shown that the above equations can be solved exactly:

$$W_k(t) = \frac{(\Gamma t)^k}{k!} W_0(t) \tag{12}$$

with $W_0(t) = \exp(-\Gamma t)$. The solution (12) allows one to derive the expressions for various observables. Defining the connectivity $\mathcal{K}$ of this network as the number of the elements in the first set $\mathcal{M}_1$, in [54] the following approximate expression has been obtained,

$$N_{\rm pc}(t) = \exp\left[2\Gamma(1 - \frac{1}{\sqrt{\mathcal{K}}})t\right]. \tag{13}$$

It should be stressed that the analogy with an infinitely large 'tree' is correct in the thermodynamic limit only. For a finite Hilbert space, as in our case, the number of the effective subsets $\mathcal{M}_k$ is finite. As a result, as $t \to \infty$ each of the probabilities $W_k(t)$ converges to a non-zero value. Moreover, the set of equation (11) is

practically restricted by a few sets (in our simulations, by $W_1(t)$ and $W_2(t)$ only, since the number of elements in $\mathcal{M}_2$ is already of the same order as the dimension of the total Hilbert space). For the case of a small number of subsets, in reference [1] the equation (11) have been modified and used to explicitly obtain an extremely detailed quench dynamics. In this case one can show that, on an intermediate time scale,

$$N_{\rm pc}(t) \approx \exp(2\Gamma t), \tag{14}$$

which coincides with equation (13) for large $\mathcal{K}$ values. From the above analysis one can see that the key parameter in the quench dynamics is the parameter Γ. This parameter is closely related to the width of the LDoS. Indeed, the LDoS is defined by,

$$F_{k_0}(E) = \sum_{\alpha} |C^{\alpha}_{k_0}|^2 \delta(E - E^{\alpha}), \tag{15}$$

where $|k_0\rangle$ is an eigenstate of H_0. Thus, it is obtained by the projection of the initial state $|k_0\rangle$ onto the eigenstates of H. The concept of LDoS is extremely important in the analysis of the dynamical properties of many-body systems. The Fourier transform of the LDoS determines the survival probability of an initially excited many-body state, and it is effectively used in the study of fidelity in many applications. In particular, the inverse width $1/\Gamma$ of LDoS gives the characteristic time scale, which is associated with the depletion of the initial state, thus representing an early stage of thermalization [42]. Initially introduced in atomic [55] and widely used in nuclear physics [56], it also serves as an important characteristic in other physical applications. As shown in many different papers (see for instance [57] and references therein), for systems with well defined classical limits, a classical analog of the LDoS can be defined and directly computed from the Hamilton equations of motion.

For isolated systems of interacting particles, described by a Hamiltonian $H = H_0 + V$, the form of LDoS changes on increasing the interaction strength V [18]. If for a weak, but not negligible, interaction the LDoS is typically a Lorentzian (apart from the tails which are due to the finite width of the energy spectrum), for a strong interaction (i.e. when the interaction energy becomes of the same order of the non-interacting one) its form becomes close to a Gaussian. Correspondingly, the width Γ of the LDoS can be estimated either using the Fermi golden rule, $\Gamma \approx 2\pi V^2 \rho_f$ where ρ_f is the density of the many-body states directly connected by V, or by the square root of the variance of LDoS, $\sigma = \sqrt{\sum H^2_{ij}}$ for $i \neq j$. When studying the TBRI model, this crossover was found to serve as the condition for the onset of strong quantum chaos, defined in terms of a pseudo-random structure of many-body eigenstates. For this reason, instead of Γ in our case one can use σ since the latter is much easier to estimate than the former. Thus, when comparing our data in figures 4 and 8 with the predicted exponential dependence (14), we use the following expression:

$$\Gamma^2 = \sum_{k \neq j_0} H^2_{k,j_0}. \tag{16}$$

As will be shown below, the simple expression (14) nicely corresponds to numerical data demonstrating the exponential increase of $N_{\rm pc}$ in time.

Now let us discuss another important characteristic of the relaxation for finite systems, namely, the time scale over which the exponential growth of $N_{\rm pc}$ lasts. To do that, we have to estimate the saturation value $\overline{N^{\infty}_{\rm pc}}$ of $N_{\rm pc}$ after the relaxation of the system to equilibrium. This value, can be obtained by the time average performed after the saturation time t_s,

$$[\ \overline{N^{\infty}_{\rm pc}}\ ]^{-1} = \lim_{T\to\infty} \frac{1}{T - t_s} \int_{t_s}^{T} {\rm d}t\ [N_{\rm pc}(t)]^{-1}. \tag{17}$$

An analytical expression, assuming non-degenerate energy levels, in terms of the eigenstates can be written as,

$$\overline{N^{\infty}_{\rm pc}} = \left[2 \sum_k (P^d_k)^2 - \sum_{\alpha} |C^{\alpha}_{k_0}|^4 \sum_k |C^{\alpha}_k|^4 \right]^{-1}. \tag{18}$$

This expression determines the total number of non-interacting many-body states inside the energy shell, excited in the process of equilibration.

Following [1], let us estimate the average value of $N_{\rm pc}$ after the relaxation, for the situation when the eigenstates are strongly chaotic. First of all let us notice that the second term in the rhs of equation (18) is roughly $1/\mathcal{D}$ times smaller than the first one, where $\mathcal{D}$ is the dimension of the many-body Hilbert space.

This can be seen by taking uncorrelated components $C_k^\alpha \simeq (1/\sqrt{\mathcal{D}})e^{i\xi_{\alpha,k}}$, where $\xi_{\alpha,k}$ are random numbers. Thus, one gets,

$$2\sum_k (P_k^d)^2 = 2\sum_{\alpha,\beta,k} |C_{k_0}^\alpha|^2 |C_k^\alpha|^2 |C_{k_0}^\beta|^2 |C_k^\beta|^2 \simeq \frac{\mathcal{D}^3}{\mathcal{D}^4} \simeq \frac{1}{\mathcal{D}}, \tag{19}$$

while

$$\sum_{\alpha,k} |C_{k_0}^\alpha|^4 |C_k^\alpha|^4 \simeq \frac{\mathcal{D}^2}{\mathcal{D}^4} \simeq \frac{1}{\mathcal{D}^2} \tag{20}$$

As a result (taking the first of the above terms only), we arrive at the estimate,

$$\left[\overline{N_{\rm pc}^\infty}\right]^{-1} \simeq 2\sum_k (P_k^d)^2. \tag{21}$$

Next, we assume a Gaussian shape for (i) the LDoS, (ii) the density of states for H_0, and (iii) the density of states of H. These are realistic assumptions for chaotic many-body systems with random two-body interactions, such as the TBRI model close to the middle of the energy spectrum. Obviously, in the tails of the spectrum the Gaussian approximation is not valid, see figure 2. Since our interest is in the energy region far from the bottom of the spectrum, our assumptions are valid, at least when we are interested in global characteristics of the dynamics, which in the first line depends on the width of the above shapes, and not on their details.

(a) For the LDoS we then assume

$$F_{k_0}(E) \simeq \frac{1}{\Gamma\sqrt{2\pi}} \exp\left\{-\frac{(E-\mathcal{E}_{k_0})^2}{2\Gamma^2}\right\}, \tag{22}$$

where Γ is the width of the LDoS and $\mathcal{E}_{k_0}$ is the energy of the non-interacting state. We also assume that Γ is independent of k_0. Note that the LDoS is normalized, $\int F_k(E)\mathrm{d}E = 1$.

(b) The Gaussian shape for the non-interacting density of states $\rho_0(E)$ of width σ_0 is written as

$$\rho_0(E) = \frac{\mathcal{D}}{\sigma_0\sqrt{2\pi}} \exp\left\{-\frac{E^2}{2\sigma_0^2}\right\}. \tag{23}$$

(c) The Gaussian density of states, characterized by a width σ, is such that

$$\rho(E) = \frac{\mathcal{D}}{\sigma\sqrt{2\pi}} \exp\left\{-\frac{E^2}{2\sigma^2}\right\}, \tag{24}$$

where for simplicity we set the middle of the spectrum at the energy $E = 0$. Both densities of states are normalized to the dimension of the Fock space,

$$\int \rho(E)\mathrm{d}E = \int \rho_0(E_0)\ \mathrm{d}E_0 = \mathcal{D}.$$

Numerical data confirm the Gaussian form of $\rho(E_0)$ and $\rho(E)$, for the TBRI model in the middle of the spectrum, see figure 2. As one can see, due to the interaction the energy spectrum increases its total width.

The above assumptions imply that in the continuum, one has

$$\begin{aligned}\sum_\alpha |C_{k_0}^\alpha|^2 |C_k^\alpha|^2 &\simeq \int \mathrm{d}E\, \rho(E)^{-1} F_k(E) F_{k_0}(E) \\ &= \frac{\sigma^2\Gamma^{-1}\mathcal{D}^{-1}}{\sqrt{2\sigma^2-\Gamma^2}} \exp\left\{-\frac{(\mathcal{E}_k)^2+(\mathcal{E}_{k_0})^2}{2\Gamma^2} + \frac{(\mathcal{E}_k+\mathcal{E}_{k_0})^2}{2\Gamma^2(2\sigma^2-\Gamma^2)}\right\} \equiv \mathcal{G}_{k_0}(\mathcal{E}_k)\end{aligned} \tag{25}$$

which is defined only for $2\sigma^2 > \Gamma^2$. We can then approximate

$$[\,\overline{N_{pc}^\infty}\,]^{-1} \simeq 2\sum_k (P_k^d)^2 \simeq 2\int \mathrm{d}E\, \rho_0(E)\mathcal{G}_{k_0}^2(E). \tag{26}$$

Taking into account that $\sigma_0^2 = \sigma^2 - \Gamma^2$, equation (26) gives

$$\overline{N_{\rm pc}^\infty} = C_1 \frac{\mathcal{D}\Gamma}{\sigma} e^{-\mathcal{E}_{k_0}^2/\Gamma^2} \tag{27}$$

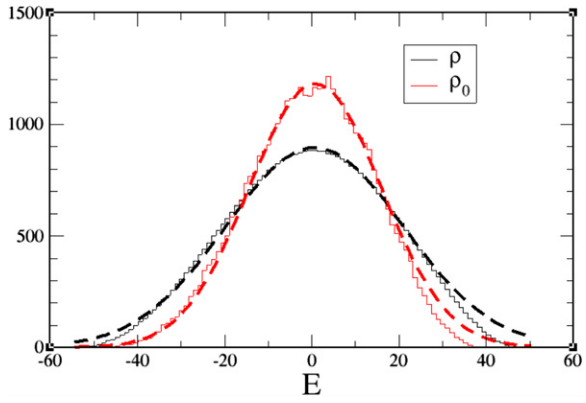

Figure 2. Histograms stands for interacting (black) and non-interacting (red) density of states for a system of $N = 8$ bosons in $M = 11$ single particle energy levels. Interaction strength is $v = 0.4$. The effective energy width of the Hamiltonians are: $\Delta_H = 98.78$ and $\Delta_{H_0} = 83.32$. Dashed lines are the Gaussian fit in the central region of the energy spectrum.

with $C_1 = \sqrt{1/2 - \Gamma^2/4\sigma^2}$.

The time t_s, determining the onset of the saturation, can be estimated from the relation,

$$\exp(2\Gamma t_s) \approx \overline{N_{\rm pc}^{\infty}}. \tag{28}$$

Considering the case for which $M \simeq 2N$, one gets an estimate for the maximal time [1]

$$t_s \approx \frac{N}{\Gamma}. \tag{29}$$

This is one of the important results, obtained in the frame of the discussed approach. As one can see, the characteristic time t_s is N times larger than the time $t_\Gamma \approx 1/\Gamma$ describing the early decrease of the return probability. The key point is that the time t_Γ has to be associated only with an initial process towards the true thermalization. In contrast, the latter emerges when the flow of probability fills *all* the subsets W_k that create the energy shell available in the thermalization process. This result can have important implications for addressing other issues such as the scrambling of information and the quantum butterfly effect.

4. Thermodynamic entropy versus diagonal entropy

Now let us discuss an important relation which has been discovered by analyzing the quench dynamics leading to thermalization. This relation links two entropies, $S_{\rm th}$ and $S_{\rm diag}$. Here

$$S_{\rm th} = \ln\ \overline{N_{\rm pc}^{\infty}} \tag{30}$$

is the thermodynamic entropy characterizing the system *after* its relaxation to equilibrium and $\overline{N_{\rm pc}^{\infty}}$ is the average number of basis states (eigenstates of H_0) in the stationary distribution. This number can be associated with the occupied 'volume' $\mathcal{V}_s(E)$ of the Hilbert space :

$$\mathcal{V}_s(E) \simeq \overline{N_{\rm pc}^{\infty}}\delta_0, \tag{31}$$

where $\delta_0 = \Delta_{H_0}/\mathcal{D}$ is the non-interacting energy spacing, Δ_{H_0} is the effective width of the energy spectrum of H_0 and $\mathcal{D}$ is the dimension of the many-body Hilbert space.

As for the diagonal entropy $S_{\rm diag}$, discussed in view of its relation to the Von Neumann entropy [58], it is given by,

$$S_{\rm diag} = -\sum_{\alpha} |C_{k_0}^{\alpha}|^2\ \ln |C_{k_0}^{\alpha}|^2. \tag{32}$$

Note that the diagonal entropy is the Shannon entropy of the set of probabilities $w_{k_0}(E^\alpha) = |C_{k_0}^{\alpha}|^2$ obtained by the projection of the non-interacting state $|k_0\rangle$ of H_0 onto the eigenstates of H. With the Shannon entropy we can built the entropic localization length

$$\ell_H = \exp\left(S_{\rm diag}\right), \tag{33}$$

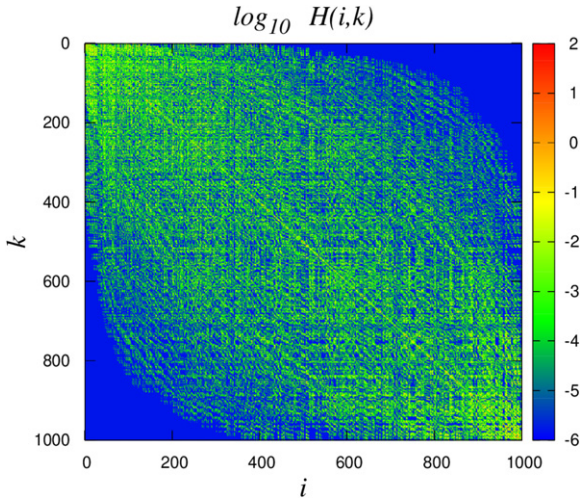

Figure 3. Global structure of the Hamiltonian matrix for the TBRI model with $N = 4$ particles, $M = 11$ momentum states and interaction strength $v = 0.4$.

giving the number of eigenstates of H excited by the initial basis state [54]. Thus, the volume occupied by the initial state is $\mathcal{V}_{\rm i}(E) \simeq \ell_H \delta$, where δ is the energy spacing estimated as $\delta \simeq \Delta_H/\mathcal{D}$. Since the two volumes are equal, $N_{\rm pc}^{\infty}\Delta_{H_0} = \ell_H \Delta_H$, we arrive at the following relation:

$$S_{\rm th} = S_{\rm diag} + \ln(\Delta_H/\Delta_{H_0}), \tag{34}$$

where Δ_H and Δ_{H_0} are the widths of the energy spectra of H and H_0, respectively. A similar correction due to the difference between Δ_H and Δ_{H_0} also appeared in other context [59].

4.1. Two-body random interaction model

The TBRI model is characterized by the Hamiltonian of N interacting bosons occupying M single-particle levels,

$$H = \sum \epsilon_s \, a_s^{\dagger} a_s + \sum V_{s_1 s_2 s_3 s_4} \, a_{s_1}^{\dagger} a_{s_2}^{\dagger} a_{s_3} a_{s_4}, \tag{35}$$

in which the single-particle levels are specified by random energies ϵ_s with mean spacing $\langle \epsilon_s - \epsilon_{s-1} \rangle = 1$ setting the energy scale. This model belongs to the class of random models since the two-body matrix elements $V_{s_1 s_2 s_3 s_4}$ are random Gaussian entries with zero mean and variance v^2. Originally suggested to describe systems with Fermi particles, recently the TBRI model has been applied to randomly interacting bosons [26–29]. As mentioned above, the Hamiltonian matrix H has a band-like form and has many zero off-diagonal elements, due to the two-body nature of the inter-particle interaction V. It is also worthwhile to mention that being constructed from random entries $V_{s_1 s_2 s_3 s_4}$, the many-body matrix elements are slightly correlated since some of them are constructed from the same two-body matrix elements. How important are these tiny correlations, have been studied analytically and numerically in reference [60]. The typical structure of the Hamiltonian matrix H is shown in figure 3.

The wave packet dynamics in the non-interacting basis $|k\rangle$ after switching on the interaction V was numerically analyzed after finding all many-body eigenstates of H and their energy eigenvalues. As one can see, the numerical study is strongly restricted by the number of particles N and the numbers M of single-particle states since the total size of the Hamiltonian matrix increases exponentially with both N and M. In our study we have mainly considered the case when $M \approx 2N$, which is akin to the study of one-dimensional lattices with M sites and N Fermi-particles. As is known, in many aspects some of the observables have the same properties when both N and M increase, keeping the ratio N/M fixed.

Our interest is in the time dependence of the number of principal components $N_{\rm pc}(t)$ in the wave function considered in the basis of H_0. As we discussed in the previous sections, the system is initially prepared in a particular non-interacting state $|k_0\rangle$, which determines the quench dynamics. Having all eigenstates and eigenvalues, we obtain the number $N_{\rm pc}(t)$ as is shown in figure 4. For sake of completeness we also plot in the same figure the curve $2\Gamma t$ corresponding to the analytical prediction obtained beyond an initial time scale on which the perturbation theory is valid. As one can see, this prediction is fully confirmed by numerical data. Now, in order to check the relation between the diagonal and thermodynamic entropies, one needs to have an accurate estimate of the diagonal entropy in the same way as we get equation (27). Let

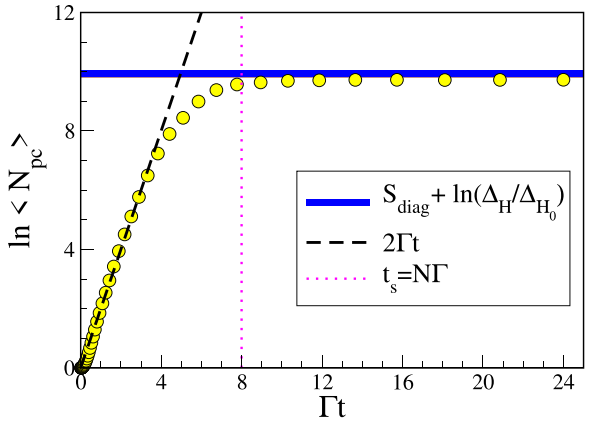

Figure 4. Time dependence of $\ln\langle N_{\rm pc}\rangle$ for the TBRI model. The average has been done over 5 disorder realizations. The initial state $|k_0\rangle$ has all $N = 8$ particles in the 5th single particle energy level. The total number of available energy levels is $M = 11$, the dimension of the Hilbert space $\mathcal{D} = 43758$ and the interaction strength is $v = 0.4$. The horizontal blue thick line represents the normalized diagonal entropy $S^{k_0}_{\rm diag} + \ln(\Delta_H/\Delta_0)$, with the thickness corresponding to one standard deviation due to different realizations of the disorder. The dashed line corresponds to $2\Gamma t$, where Γ is the width of the LDoS associated with the initial non-interacting state and averaged over the 5 disordered realizations. On horizontal axis we used the dimensionless time Γt. Vertical dotted line represents the estimate $\Gamma t_s = N$, where $N = 8$ is the number of particles.

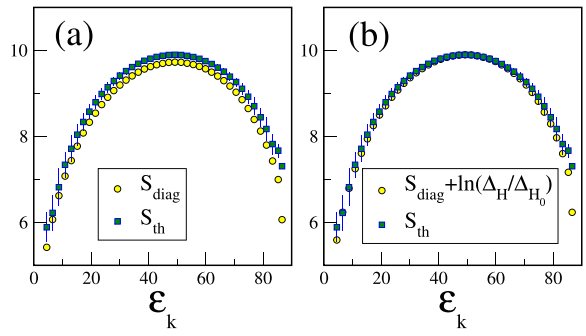

Figure 5. (a) TBRI: thermodynamic entropy $S_{\rm th} = \ln\ N^{\infty}_{\rm pc}$ and diagonal entropy $S_{\rm diag}$ vs the energy of the initial state $\mathcal{E}_k$. Here we took $N = 8$ bosons in $M = 11$ single-particle energy levels. Interaction strength $v = 0.4$. (b) the same but we added the correction to the diagonal entropy due to the different spectral widths of H and H_0. Average over close energies has been performed. Error bars indicate one standard deviation.

us start with the expression given in equation (32), associated with the initial state $|k_0\rangle$ using the same approximations as above,

$$S_{\rm diag} \simeq -\int {\rm d}E F_{k_0}(E)\ \ln[F_{k_0}(E)] + \int {\rm d}E F_{k_0}(E)\ \ln[\rho(E)]. \tag{36}$$

Taking only the dominant contribution one gets

$$\ell_{\rm diag} \equiv \exp\{S_{\rm diag}\} = C_2 \frac{\mathcal{D}\Gamma}{\sigma} {\rm e}^{-\mathcal{E}^2_{k_0}/\Gamma^2} \tag{37}$$

with $C_2 = \exp[(1 - \Gamma^2/\sigma^2)/2]$. Comparing equation (27) with equation (37) one finally gets,

$$\overline{N^{\infty}_{\rm pc}} = (C_1/C_2)\ell_{\rm diag}. \tag{38}$$

This proves that the global functional dependence of both $\overline{N^{\infty}_{\rm pc}}$ and $\ell_{\rm diag}$ on the initial energy $\mathcal{E}_{k_0}$ is the same and they turn out to be proportional one to each other.

In order to check both the consistency of our physical argument and of the relation (38) we considered for the whole set of initial energies $\mathcal{E}_{k_0}$ the two entropies, see figure 5 panel (a). As one can see they have the same dependence even if they are slightly shifted due to the variation in the size of the energy spectra. Taking into account the correction due to the different spectral widths of H and H_0, we can see that the two entropies are pretty much the same, apart from small deviations at the edge of the spectrum where eigenstates are expected to be non-chaotic, see panel (b) of the same figure.

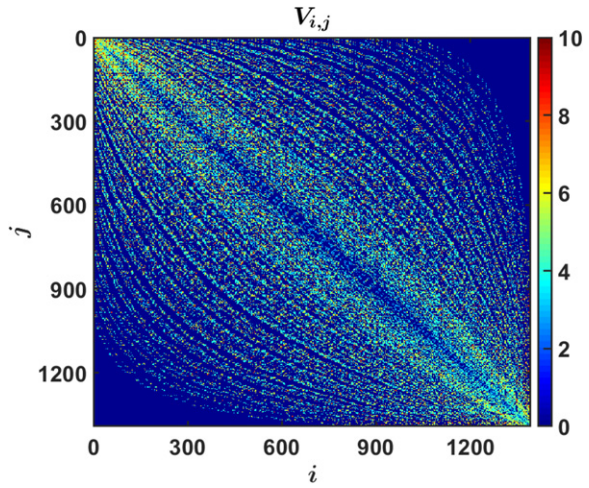

Figure 6. t-LL model: structure of the Hamiltonian matrix for a system with $N = 5$ particles and $\ell = 17$ momentum states and fixed total momentum $\mathcal{M} = 1$. Here we set $g = 1$ and only off-diagonal matrix elements are shown.

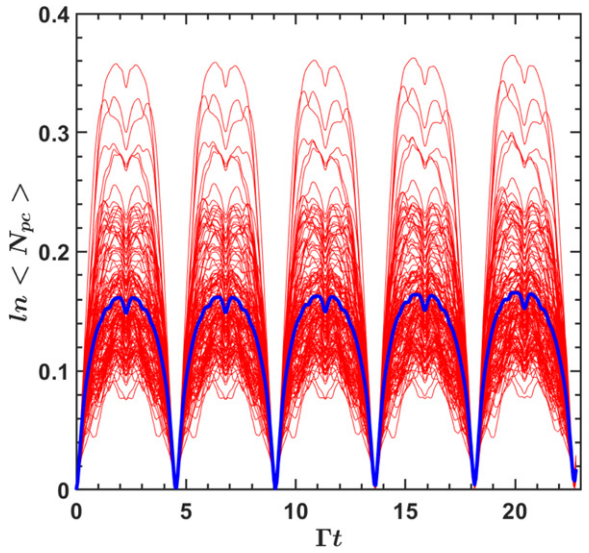

Figure 7. Time dependence of $\ln\langle N_{\rm pc}\rangle$ for the t-LL model for weak interaction (MF regime). On x-axis we put the dimensionless time Γt where Γ is the width of the LDoS averaged over the degenerate initial states. The average (blue curve) has been done over all initial degenerate states having the same energy E_0 close to the band center (with $j_0 \approx 4050$). Here we considered $N = 9$ particles in $\ell = 13$ momentum levels, $n/g = 10$, for a fixed total momentum $\mathcal{M} = 1$ (the matrix size is 8122). The normalized diagonal entropy $S_{\rm diag} + \ln(\Delta_H/\Delta_{H_0}) = 2.75 \pm 1$ does not correspond to the equilibrium value since for this interaction strength the eigenstates involved in the dynamics are not chaotic.

4.2. Truncated LL model (t-LL)

The Hamiltonian of the Lieb–Liniger model with N bosons occupying a ring of length L, in dimensionless units can be written as,

$$H = \sum_s \epsilon_s \hat{n}_s + \frac{g}{L}\sum_{s,q,p,r} \hat{a}_s^\dagger \hat{a}_q^\dagger \hat{a}_p \hat{a}_r \delta(s+q-p-r). \tag{39}$$

Here g is the parameter determining the strength of interaction between particles, and the single-particle energy levels (for non-interacting bosons) are given by

$$\epsilon_s = 4\pi^2 s^2/L^2.$$

The $\delta-$function in equation (39) indicates the momentum conservation of the two-body interaction. Below, the single-particle states $|\phi_s\rangle$ are labeled according to their momentum $s = 0, \pm 1, \pm 2, \ldots$. From them, the many-body non-interacting states $|j\rangle = |\ldots n_{-s} \ldots n_0, \ldots, n_s \ldots\rangle$ have been built, where n_s indicates the number of particles in the sth momentum level. In our numerical study, in order to fit physical experiments, we consider a finite number N of particles occupying a finite number $\ell = 2M + 1$ of

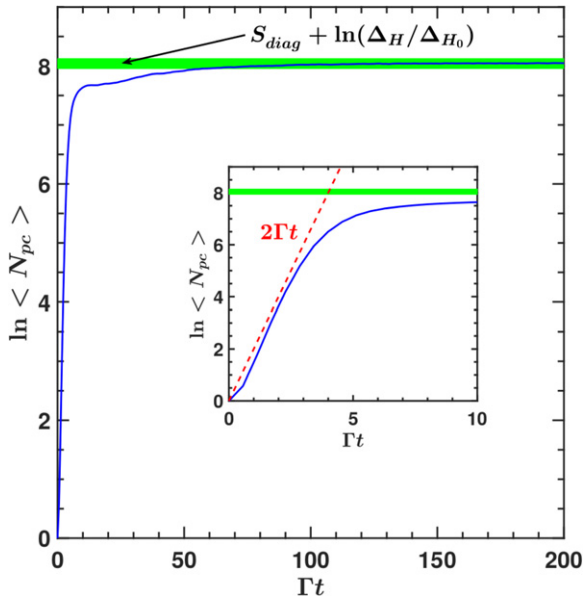

Figure 8. Time dependence of $\ln\langle N_{\rm pc}\rangle$ for the t-LL model. On x-axis we put the dimensionless time Γt where Γ is the width of the LDoS averaged over the degenerate initial states. The average has been done over all initial degenerate states having the same energy E_0 close to the band center (with $j_0 \approx 4050$). Inset: the early stage of the evolution of $\ln\langle N_{\rm pc}\rangle$, in comparison with linear dependence $2\Gamma t$ (red dashed line). Here we considered $N = 9$ particles in $\ell = 13$ momentum levels, $n/g = 0.5$, for a fixed total momentum $\mathcal{M} = 1$ (the matrix size is 8122). Horizontal green thick line represents the normalized diagonal entropy $S_{\rm diag} + \ln(\Delta_H/\Delta_{H_0})$, the thickness corresponds to one standard deviation due to different initial states. In computing Δ_H and Δ_{H_0} we excluded a number of energies close to the band edges.

single-particle momentum states. Note that the total number of single-particle energies ϵ_s is $M + 1$ since the states with momentum $\pm s$ are degenerate. We choose N and $2M$ to be approximately the same, in analogy with the case considered above for the TBRI model. A rough estimate, $n = N/L \sim g$, for the crossover from the MF to the TG regime in connection with quantum chaos, is discussed in [61]. The structure of the Hamiltonian matrix at some fixed total momentum value $\mathcal{M}$ is shown in figure 6 and as one can see it is very similar to that presented in figure 3 for the TRBI model.

Our numerical study of the quench dynamics of the t-LL model demonstrates that $N_{\rm pc}(t)$ oscillates in time in the MF regime ($n/g \gg 1$) as shown in figure 7. In contrast, it grows exponentially fast in the TG regime ($n/g \lesssim 1$, see figure 8), after a short time where, due to the standard perturbation theory, the time-dependence is quadratic in time. This exponential growth lasts up to some time t_s after which a clear saturation of $N_{\rm pc}$ emerges, together with irregular fluctuations around its mean value. In order to reduce these fluctuations which are due to different initial conditions (various values of j_0), we have performed the average $\langle N_{\rm pc}\rangle$ over all those initial non-interacting basis states with the same energy.

First, the numerical data clearly manifest a very good correspondence to the analytical estimates of the exponential increase of $N_{\rm pc}(t)$ occurring for $t \ll t_s$. Second, the relaxation time t_s roughly corresponds to the estimate $t_s \approx N/\Gamma$ (specifically, to $\Gamma t_s \approx N$ with $N = 9$). Finally, the relation (34) between the diagonal and thermodynamic entropies holds with a very good accuracy. All these results are highly non-trivial since they are obtained for the t-LL model which is non-random. Specifically, one can show that the non-diagonal matrix elements of the total Hamiltonian are strongly correlated. For the case shown in figure 8 diagonal and off-diagonal Hamiltonian matrix elements take the values from a set with very few elements, as one can see from the plots shown in figure 9. It is important to note that the validity of our analytical expression holds also in this case where the non-interacting density of states is a set of $\delta-$functions (and certainly not a Gaussian).

5. Summary

We have studied two different models, the TBRI model with random two-body interaction and the truncated LL model (t-LL) with a finite number of particles in a finite number of momentum states which is originated from the completely integrable Lieb–Liniger model. By studying the quench dynamics in the region where the many-body eigenstates can be considered as strongly chaotic, we have found that the time evolution of both models is quite similar to that recently found for the random TBRI, as well as for the deterministic XXZ model of interacting 1D spins-1/2 [19, 20]. Specifically, the number of components in

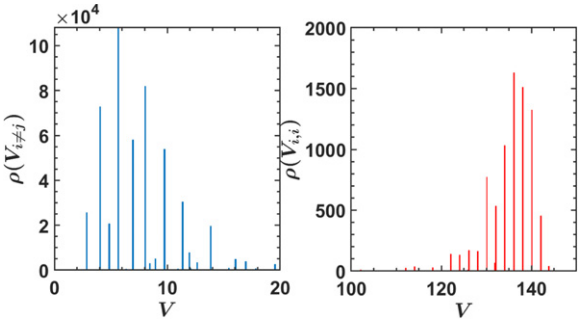

Figure 9. Truncated LL model (t-LL). Left panel: distribution of off-diagonal elements $\rho(V_{i,j})$ for the Hamiltonian matrix equation (39). Right panel: distribution of diagonal matrix elements $\rho(V_{i,i})$. Here we considered $N = 9$ particles in $\ell = 13$ momentum levels and $g = 1$.

the wave packets evolving in the Hilbert space, increases exponentially in time with a rate given by twice the width of the LDoS related to the initial state of the non-interacting many-body Hamiltonian H_0. This growth lasts approximately until the saturation time t_s which is much larger than the inverse width of the LDoS characterizing the initial decay of the survival probability. Both the rate of the exponential increase and the characteristic time t_s for the onset of equilibration, nicely correspond to our semi-analytically estimates.

By studying the process of relaxation of the system to the equilibrium, we have discovered a remarkable relation between the thermodynamic entropy $S_{\rm th}$ (defined in terms of the number of principal components $N_{\rm pc}$ in the wave function) of the system *after the equilibration*, and the diagonal entropy $S_{\rm diag}$ related to an *initial many-body state*. This relation (34) establishes a direct link between statistical and thermodynamical properties, and seems to be generic, valid for both deterministic and random many-body systems. Recently, another relation between the diagonal entropy and the GGE entropy was found in a fully integrable 1D Ising model in a transverse magnetic field [62, 63]. Thus, a further study of the relevance of the diagonal entropy to the thermodynamic properties of many-body systems seems to be very important, especially, in view of possible experimental studies of the onset of thermalization in isolated systems.

Acknowledgments

FB acknowledges support by the Iniziativa Specifica INFN-DynSysMath and FMI acknowledges financial support from CONACyT (Grant No. 286633). This publication has been financially supported by the Catholic University of Sacred Heart within the program of promotion and diffusion of scientific research. Research has been financially supported by Ministero dell'Istruzione, dell'Università e della Ricerca within the project PRIN 20172H2SC4.

ORCID iDs

Samy Mailoud https://orcid.org/0000-0001-6173-5762
Fausto Borgonovi https://orcid.org/0000-0002-9730-1189
Felix M Izrailev https://orcid.org/0000-0003-0326-2017

References

[1] Borgonovi F, Izrailev F M and Santos L F 2019 Exponentially fast dynamics in the Fock space of chaotic many-body systems *Phys. Rev.* E **99** 010101(R)
[2] Horoi M, Zelevinsky V and Brown B A 1995 Chaos vs thermalization in the nuclear shell model *Phys. Rev. Lett.* **74** 5194
[3] Zelevinsky V, Brown B A, Frazier N and Horoi M 1996 The nuclear shell model as a testing ground for many-body quantum chaos *Phys. Rep.* **276** 85
[4] Flambaum V V and Izrailev F M 1997 Statistical theory of finite Fermi systems based on the structure of chaotic eigenstates *Phys. Rev.* E **56** 5144
[5] Zelevinsky V 1996 Quantum chaos and complexity in nuclei *Annu. Rev. Nucl.* **46** 237
[6] Borgonovi F, Guarneri I, Izrailev F M and Casati G 1998 Chaos and thermalization in a dynamical model of two interacting particles *Phys. Lett.* A **247** 140
[7] Gribakin G F, Gribakina A A and Flambaum V V 1999 Quantum chaos in multicharged ions and statistical approach to the calculation of electron-ion resonant radiative recombination *Aust. J. Phys.* **52** 443

[8] Rigol M, Dunjko V and Olshanii M 2008 Thermalization and its mechanism for generic isolated quantum systems *Nature* **452** 854
[9] Polkovnikov A, Sengupta K, Silva A and Vengalattore M 2011 Colloquium: Nonequilibrium dynamics of closed interacting quantum systems *Rev. Mod. Phys.* **83** 863
[10] D'Alessio L, Kafri Y, Polkovnikov A and Rigol M 2016 From quantum chaos and eigenstate thermalization to statistical mechanics and thermodynamics *Adv. Phys.* **65** 239
[11] Luitz D J and Lev Y B 2016 Anomalous hermalization in ergodic systems *Phys. Rev. Lett.* **117** 170404
[12] Abanin D A, Altman E, Bloch I and Serbyn M 2019 Colloquium: many-body localization, thermalization, and entanglement *Rev. Mod. Phys.* **91** 021001
[13] Greiner M, Mandel O, Hansch T W and Bloch I 2002 Collapse and revival of the matter wave field of a Bose–Einstein condensate *Nature* **419** 51
[14] Trotzky S *et al* 2012 Probing the relaxation towards equilibrium in an isolated strongly correlated one-dimensional Bose gas *Nat. Phys.* **8** 325
[15] Gring M *et al* 2012 Relaxation and prethermalization in an isolated quantum system *Science* **337** 1318
[16] Kaufman A M *et al* 2016 Quantum thermalization through entanglement in an isolated many-body system *Science* **353** 794
[17] Nandkishore R and Huse D A 2015 Many-body localization and thermalization in quantum statistical mechanics *Annu. Rev. Condens. Matter Phys.* **6** 15
[18] Borgonovi F, Izrailev F M, Santos L F and Zelevinsky V G 2016 Quantum chaos and thermalization in isolated systems of interacting particles *Phys. Rep.* **626** 1
[19] Santos L F, Borgonovi F and Izrailev F M 2012 Onset of chaos and relaxation in isolated systems of interacting spins: energy shell approach *Phys. Rev.* E **85** 036209
[20] Santos L F, Borgonovi F and Izrailev F M 2012 Chaos and statistical relaxation in quantum systems of interacting particles *Phys. Rev. Lett.* **108** 094102
[21] Wigner E P 1955 Characteristic vectors of bordered matrices with infinite dimensions *Ann. Math.* **62** 548
Wigner E P 1957 Characteristics vectors of bordered matrices with infinite dimensions II *Ann. Math.* **65** 203
Wigner E P 1958 On the distribution of the roots of certain symmetric matrices *Ann. Math.* **67** 325
[22] Dyson F J 1962 Statistical theory of the energy levels of complex systems I *J. Math. Phys.* **3** 140
Dyson F J 1962 Statistical theory of the energy levels of complex systems II *J. Math. Phys.* **3** 157
Dyson F J 1962 Statistical theory of the energy levels of complex systems III *J. Math. Phys.* **3** 166
[23] French J B and Wong S S M 1970 Validity of random matrix theories for many-particle systems *Phys. Lett.* B **33** 449
[24] Bohigas O and Flores J 1971 Spacing and individual eigenvalue distributions of two-body random Hamiltonians *Phys. Lett.* B **35** 383
Bohigas O and Flores J 1971 Two-body random Hamiltonian and level density *Phys. Lett.* B **34** 261
[25] Brody T A, Flores J, French J B, Mello P A, Pandey A and Wong S S M 1981 Random-matrix physics: spectrum and strength fluctuations *Rev. Mod. Phys.* **53** 385
[26] Benet L and Weidenmueller H A 2003 Review of the k-body embedded ensembles of Gaussian random matrices *J. Phys. A: Math. Gen.* **36** 3569
[27] Chavda N D, Kota V K B and Potbhare V 2012 Thermalization in one- plus two-body ensembles for dense interacting boson systems *Phys. Lett.* A **376** 2972
[28] Kota V K B and Chavda N D 2018 Embedded random matrix ensembles from nuclear structure and their recent applications *Int. J. Mod. Phys.* E **27** 1830001
[29] Vyas M and Kota V K B 2019 Quenched many-body quantum dynamics with k-body interactions using q-Hermite polynomials *J. Stat. Mech.* 103103
[30] Kota V K B 2014 *Embedded Random Matrix Ensembles in Quantum Physics* (Heidelberg: Springer)
[31] Sachdev S and Ye J 1993 Gapless spin-fluid ground state in a random quantum Heisenberg magnet *Phys. Rev. Lett.* **70** 3339
[32] Kitaev A 2015 A simple model of quantum holography, KITP Entangled15 http://online.kitp.ucsb.edu/entangled15
[33] Jia Y and Verbaarschort J J M 2019 Spectral fluctuations in the Sachdev-Ye-Kitaev model (arXiv:1912.11923 [hep-th])
[34] Shenker S H and Stanford D 2014 Black holes and the butterfly effect *J. High Energy Phys.* JHEP03(2014)067
[35] Cotler J, Hunter-Jones N, Liu J and Yoshida B 2017 Chaos, complexity, and random matrices *J. High Energy Phys.* JHEP11(2017)048
[36] Blake M, Davison R A, Grozdanov S and Liu H 2018 Many-body chaos and energy dynamics in holography *J. High Energy Phys.* JHEP10(2018)035
[37] Larkin A and Ovchinnikov Y N 1969 Quasiclassical method in the theory of super-conductivity *JETP* **28** 1200–5
[38] Maldacena J, Shenker S H and Stanford D 2016 A bound on chaos *J. High Energy Phys.* JHEP16(2016)106
[39] Rozenbaum E B, Ganeshan S and Galitski V 2017 Lyapunov exponent and out-of-time-ordered correlator's growth rate in a chaotic system *Phys. Rev. Lett.* **118** 086801
[40] Swingle B 2018 Unscrambling the physics of out-of-time- order correlators *Nat. Phys.* **14** 988
[41] Rossini D, Suzuki S, Mussardo G, Santoro G E and Silva A 2010 Long time dynamics following a quench in an integrable quantum spin chain: local versus nonlocal operators and effective thermal behavior *Phys. Rev.* B **82** 144302
[42] Borgonovi F, Izrailev F M and Santos L F 2019 Timescales in the quench dynamics of many-body quantum systems: participation ratio versus out-of-time ordered correlator *Phys. Rev.* E **99** 052143
[43] Lieb E H and Liniger W 1963 Exact analysis of an interacting Bose gas: I. The general solution and the ground state *Phys. Rev.* **130** 1605
[44] Lieb E H 1963 Exact analysis of an interacting Bose gas: II. The excitation spectrum **130** 1616
[45] Girardeau M 1960 Relationship between systems of impenetrable bosons and fermions in one dimension *J. Math. Phys.* **1** 516
[46] Bethe H A 1931 Zur Theorie der Metalle *Z. Phys* **71** 205
[47] Korepin V E, Bogoliubov N M and Izergin A G 1993 *Quantum Inverse Scattering Method and Correlation Functions* (Cambridge: Cambridge University Press) (https://doi.org/10.1017/CBO9780511628832)
[48] Gorlitz A *et al* 2001 Realization of Bose-Einstein condensates in lower dimensions *Phys. Rev. Lett.* **87** 130402
[49] Kinoshita T, Wenger T and Weiss D S 2004 Observation of a one-dimensional Tonks-Girardeau gas *Science* **305** 1125
[50] Paredes B *et al* 2004 Tonks–Girardeau gas of ultracold atoms in an optical lattice *Nature* **429** 377
[51] Olshanii M 1998 Atomic scattering in the presence of an external confinement and a gas of impenetrable bosons *Phys. Rev. Lett.* **81** 938

[52] The details will be published elsewhere.
[53] Robinson N J, de Klerk A J J M and Caux J-S 2019 On computing non-equilibrium dynamics following a quench (arXiv:1911.11101)
[54] Flambaum V V and Izrailev F M 2001 Entropy production and wave packet dynamics in the Fock space of closed chaotic many-body systems *Phys. Rev.* E **64** 036220
[55] Rice O K 1933 Predissociation and the crossing of molecular potential energy curves *J. Chem. Phys.* **1** 375
[56] Bohr A and Mottelson B R 1969 *Nuclear Structure* (New York: Benjamin)
[57] Izrailev F M 2001 Quantum-classical correspondence for isolated systems of interacting particles: localization and ergodicity in energy space *Phys. Scr.* **T90** 95 *Proc. of the Nobel Simposia 'Quantum Chaos Y2K'*
[58] Polkovnikov A 2011 Microscopic diagonal entropy and its connection to basic thermodynamic relations *Ann. Phys.* **326** 486
[59] Borgonovi F and Izrailev F M 2000 Classical statistical mechanics of a few-body interacting spin model *Phys. Rev.* E **62** 6475
[60] Flambaum V V, Gribakin G F and Izrailev F M 1996 Correlations within Eigenvectors and transition amplitudes in the two-body random interaction model *Phys. Rev.* E **53** 5729
[61] Berman G P, Borgonovi F, Izrailev F M and Smerzi A 2004 Irregular dynamics in a one-dimensional bose system *Phys. Rev. Lett.* **92** 030404
[62] Kormos M, Bucciantini L and Calabrese P 2014 Stationary entropies after a quench from excited states in the Ising chain *Europhys. Lett.* **107** 40002
[63] Piroli L, Vernier E, Calabrese P and Rigol M 2017 Correlations and diagonal entropy after quantum quenches in XXZ chains *Phys. Rev.* B **95** 054308